

## LINKED DIAGRAM EXPANSIONS FOR THE NUCLEAR TRANSITION MATRIX AND THE NORMALIZATION OF MODEL-SPACE WAVE FUNCTIONS\*

D.B. STOUT and T.T.S. KUO

*Physics Department, State University of New York at Stony Brook, Stony Brook, NY 11794-3800, USA*

Received 19 January 1989

(Revised 13 November 1990)

**Abstract:** A unified and relatively simple linked-diagram expansion for performing microscopic calculations of the nuclear transition matrix  $T_{fi}$  is derived. We first review a folded-diagram effective interaction theory, based on which, the model-space effective hamiltonian can be calculated from realistic nucleon-nucleon interactions. An important ingredient of this theory is the wave-function decomposition theorem which provides a convenient connection between the true and model-space wave functions. By directly making use of this theorem, a folded-diagram expansion of  $T_{fi}$  is readily obtained. Using a partial summation method, the folded diagrams of  $T_{fi}$  are then eliminated, leading to a considerably simpler expression for  $T_{fi}$ . Our formalism requires that  $T_{fi}$  must be calculated in strict consistence with the derivation of the model-space effective hamiltonian  $H^{eff}$ . The model-space wave function normalization factor contained in our  $T_{fi}$  may play an important role in "quenching" the calculated nuclear transition matrix. A simple method for evaluating this normalization factor is derived, namely it can be obtained readily from the energy derivative of the respective self-consistent eigenvalue of  $H^{eff}$ .

### 1. Introduction

In studying nuclear transitions such as electromagnetic radiations and beta decays, the basic quantity to be calculated is the transition matrix  $T_{fi} = \langle \Psi_f | T | \Psi_i \rangle$  where  $\Psi_f$  and  $\Psi_i$  denote respectively the final and initial wave functions of the nuclear system under consideration, and  $T$  is the physical transition operator. As is well known, the calculation of  $T_{fi}$  is in fact a rather difficult undertaking.

The nuclear wave functions  $\Psi_f$  and  $\Psi_i$  are complicated many-body wave functions; it is impossible to calculate them exactly. Even if they could be exactly determined, they would be too complicated to be of physical interest. For example, the complete shell-model wave function for the nucleus of  $^{18}\text{O}$ , a frequently used example for nuclear structure theories, will have 2p0h, 3p1h, all the way up to 18p16h components. To say the least, it is certainly not convenient to use such wave functions in calculating  $T_{fi}$ . To avoid the above difficulty, a commonly used procedure is to employ some model-space wave functions  $\chi_f$  and  $\chi_i$  in place of  $\Psi_f$  and  $\Psi_i$ , and then calculate the effective transition matrix  $T_{fi}^{eff} = \langle \chi_f | T^{eff} | \chi_i \rangle$ .

The model-space wave functions are generally not equal to the true nuclear wave functions. For example, a typical model-space wave function for  $^{18}\text{O}$  has only 2p0h

\* Work supported in part by US DOE Grant DE-FG02-88ER40388.

components. We formally define  $T^{\text{eff}}$  by requiring  $T_{fi}^{\text{eff}} = T_{fi}$  for certain chosen nuclear states  $f$  and  $i$  (not all). It is clear that the effective transition operator  $T^{\text{eff}}$  is in general not equivalent to the original (bare) transition operator, but contains renormalization corrections. The derivation of  $T^{\text{eff}}$  has long been an important yet difficult problem in nuclear theory. Many authors<sup>1-11)</sup> have studied this problem and made progress, but much remains to be done in order to make the basic theory for deriving and calculating  $T^{\text{eff}}$  more satisfactory and simplified.

We wish to study in the present work a unified, relatively simple, and practical method for calculating the transition matrix  $T_{fi}^{\text{eff}}$  starting from a realistic many-body nuclear hamiltonian. Our method is basically a simplification and extension of the folded diagram approach of Krenciglowa and Kuo<sup>6)</sup>. In their approach, the effective transition matrix  $T_{fi}^{\text{eff}}$  was expressed in a form of  $N/D$  where both  $N$  and  $D$  contain folded diagrams. The derivation of  $T_{fi}^{\text{eff}}$  as well as the calculation of  $N$  and  $D$  were both rather involved. In the present work, we also express  $T_{fi}^{\text{eff}}$  in a form of  $N/D$ , but we have found a considerably simpler derivation. In addition, we shall show that the folded diagrams contained in  $N$  and  $D$  can each be summed up using a partial summation method so that no folded diagrams appear in our final result, thus simplifying the calculation of  $N$  and  $D$ . A somewhat interesting byproduct of the present work is that we have derived a fairly simple method for evaluating the normalization of the model-space wave functions. As to be described later, this normalization can be conveniently calculated from the energy derivative of the respective self-consistent eigenvalue. This makes it feasible to actually evaluate the normalization of the model-space wave functions of nuclear structure calculations using a realistic nucleon-nucleon interaction. In this way, we are in a position to examine the validity of the commonly adopted practise of always normalizing the shell-model wave functions to unity. In microscopic nuclear structure calculations, it is likely that the normalization of the model-space wave function is generally less than unity as we will later discuss.

Before presenting our method, let us first introduce our notations. The nuclear hamiltonian is divided into two parts  $H = H_0 + V$  where  $H_0$  is a one-body hamiltonian,  $H_0 = \sum_q \varepsilon_q a_q^\dagger a_q$ , and  $V$  is the remaining interaction, typically taken to be two-body. The many-body eigenfunctions for  $N$  particles, and the eigenenergies of  $H$  and  $H_0$  are defined respectively by

$$H\Psi_\lambda^N = E_\lambda^N \Psi_\lambda^N, \quad (1.1)$$

$$H_0\phi_\lambda^N = W_\lambda^N \phi_\lambda^N. \quad (1.2)$$

As usual, we introduce a model-space with projection operator  $P$  and conjugate projection operator  $Q$  defined in terms of the eigenfunctions of  $H_0$ , i.e.

$$P = \sum_{k=1}^d |\phi_k^N\rangle\langle\phi_k^N|, \quad Q = 1 - P \quad (1.3)$$

where  $d$  is the dimension of the model-space. One calls states within the model-space the active states. Correspondingly,  $Q$  projects onto all states outside the model-space, henceforth known as passive states.

In this work, we divide the set of all the single-particle (s.p.) states  $\{\alpha\}$  into two disjoint subsets  $\{a\}$  and  $\{\bar{a}\}$  and call them active and passive, respectively. They are chosen such that  $\{\alpha\} = \{a\} \cup \{\bar{a}\}$  and  $\{a\} \cap \{\bar{a}\} = 0$ . We denote the elements contained in  $\{a\}$  by  $a_1, a_2, a_3, \dots$ , and those in  $\{\bar{a}\}$  by  $\bar{a}_1, \bar{a}_2, \bar{a}_3, \dots$ .

Our model-space will always be chosen to consist of an  $A$ -particle closed core state  $|c\rangle$  ( $H_0|c\rangle = W_0^A|c\rangle$ ), with  $n_p$  active valence particles and  $n_h$  active holes. That is, the model-space states are of the form

$$|\phi_k^N\rangle = \underbrace{a_1^\dagger \dots a_j^\dagger}_{n_p} \underbrace{a_l \dots a_m}_{n_h} |c\rangle \quad (1.4)$$

with  $N = A + n_v$  where  $n_v = n_p + n_h$ .

A familiar example is the model-space consisting of two neutrons in the  $0d_{1/2}$  shell with a closed  $^{16}\text{O}$  core, commonly used in nuclear structure calculations of  $^{18}\text{O}$  (see fig. 1a). When writing diagrams, particles and holes outside the model-space will be denoted by railed lines (see fig. 1b). Thus states outside the model-space will always contain at least one railed line. In the present work, we shall frequently use the example of the  $^{18}\text{O}$  nucleus to illustrate our formulae.

As discussed earlier, exact solutions of the general many-body problem of (1.1) are practically not possible. Consequently one only looks for some of its approximate

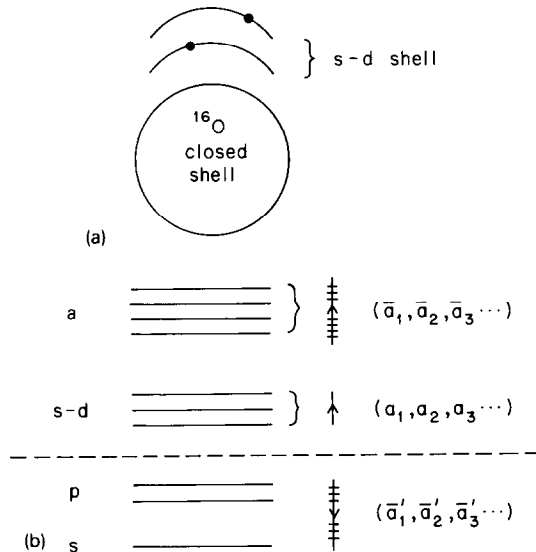


Fig. 1. (a)  $^{18}\text{O}$  two valence nucleons outside a closed  $^{16}\text{O}$  core. (b) Definition of active ( $a_1, a_2, a_3, \dots$ ) and passive ( $\bar{a}_1, \bar{a}_2, \bar{a}_3, \dots$ ) single-particle states for the  $^{18}\text{O}$  model-space.

solutions. This is usually done by first rewriting (1.1) as a model-space secular equation

$$PH^{\text{eff}}P\chi_\alpha^N = E_\alpha^N\chi_\alpha^N, \quad \alpha = 1, d, \quad (1.5)$$

and then solving this reduced many-body problem. Note that (1.5) reproduces only  $d$  eigenvalues of (1.1).  $H^{\text{eff}}$  is the effective hamiltonian which operates only within the model-space  $P$ , and a systematic derivation of it can be carried out using, for example, a folded diagram method<sup>2-13</sup>).  $\chi_\alpha^N$  is usually chosen to be the projection of  $\Psi_\alpha^N$  onto the model-space, namely

$$\chi_\alpha^N = P\Psi_\alpha^N. \quad (1.6)$$

In almost all nuclear structure calculations such as the well known shell-model calculations, one calculates only  $E_\alpha^N$  and  $\chi_\alpha^N$  of (1.5) and (1.6).

In calculating the transition matrix  $T_{\alpha\alpha'} = \langle \Psi_\alpha^N | T | \Psi_{\alpha'}^N \rangle$  we need to know, however, the true eigenfunctions  $\Psi$ . This poses a major difficulty as (1.5) only calculates  $\chi$ , and furthermore it does not determine the norm of  $\chi$ . To overcome this difficulty, we first need to carefully investigate the effective interaction theory from which the effective hamiltonian of (1.5) is derived. Then, we may understand the precise connection between  $\chi^N$  and  $\Psi^N$ . It will then be possible to calculate  $T_{\alpha\alpha'}$  starting from the model-space wave functions  $\chi_\alpha^N$  and  $\chi_{\alpha'}^N$ .

In the next section, we shall first outline the effective interaction theory on which we base our calculation of the transition matrix for open shell nuclei. Then in sect. 3, we shall derive and discuss a linked-diagram expansion for the transition matrix. A relatively simple method for determining the normalization of the model-space wave functions will also be presented there.

## 2. Effective interaction

Nuclear wave functions are almost always calculated from a model-space secular equation, and they are usually only the projection of the nuclear eigenstates onto the respective model-space. To carry out a consistent calculation of the nuclear transition matrix using these model-space wave functions, it is essential to know precisely how these model-space wave functions are derived. In this section, we describe briefly a folded-diagram effective interaction theory formulated by Kuo, Lee, and Ratcliff (KLR)<sup>12-14</sup>); it provides a general framework for deriving the model-space effective interaction as well as the model-space wave functions.

A basic step in almost all microscopic effective interaction theories is the formal construction of a true eigenstate of the many-body system starting from an unperturbed wave function. This can be carried out using either the adiabatic approach of Gell-Mann and Low<sup>14</sup>) or the complex time approach of Thouless<sup>15</sup>). To outline how it works, let us consider the open shell nucleus  $^{18}\text{O}$ . The eigenfunctions and energies of this nucleus are denoted respectively by  $\Psi_\alpha^{A+2}$  and  $E_\alpha^{A+2}$ . The ground

state energy and wave function of the core nucleus  $^{16}\text{O}$  are denoted by  $E_0^A$  and  $\Psi_0^A$  respectively. The starting point of the KLR method is that true eigenstates  $\Psi_\alpha$  can be constructed<sup>14,15)</sup> from model-space wave functions  $\rho_\alpha$

$$\frac{|\Psi_\alpha\rangle}{\langle\rho_\alpha|\Psi_\alpha\rangle} = \lim_{\eta \rightarrow 0} \frac{U_\eta(0, -\infty)|\rho_\alpha\rangle}{\langle\rho_\alpha|U_\eta(0, -\infty)|\rho_\alpha\rangle}, \quad (2.1)$$

where  $U_\eta$  is the time evolution operator. The subscript  $\eta$  indicating that an ‘‘adiabatic’’ damping factor<sup>15)</sup> has been introduced in switching on the interaction from time  $-\infty$  to 0. To obtain the above result, we assume that our model-space can be chosen in such a way that  $P\Psi_\alpha$ ,  $\alpha = 1, d$ , are linearly independent. The states  $\rho_\alpha$ , which are contained entirely within the model-space (i.e.  $P\rho_\alpha = \rho_\alpha$ ), may be referred to as the parent states. As we shall see shortly, in our formalism we never actually need to know  $\rho_\alpha$ .

We note that the state  $\lim_{\eta \rightarrow 0} U_\eta|\rho_\alpha\rangle / \langle\rho_\alpha|U_\eta|\rho_\alpha\rangle$  is only proportional to the eigenstate  $\Psi_\alpha$ . Furthermore, the denominator  $\langle\rho_\alpha|U_\eta|\rho_\alpha\rangle$  plays a very important role.  $U_\eta(0, t)|\rho_\alpha\rangle$  is by itself undefined in the limit of  $t \rightarrow -\infty$ ,  $\eta \rightarrow 0$ ; only the ratio indicated above is well defined in the limit<sup>10)</sup>. Henceforth, the  $\eta \rightarrow 0$  limit will be understood and we shall no longer explicitly write it.

We have from (2.1) that

$$H \frac{U_\eta|\rho_\alpha\rangle}{\langle\rho_\alpha|U_\eta|\rho_\alpha\rangle} = E_\alpha \frac{U_\eta|\rho_\alpha\rangle}{\langle\rho_\alpha|U_\eta|\rho_\alpha\rangle}, \quad (2.2)$$

where for brevity we have used  $U_\eta$  to denote  $U_\eta(0, -\infty)$ ; this notation will be used from now on unless specified otherwise.

To facilitate the later derivation of transition matrices, it is useful to describe and analyse in some detail the so-called decomposition theorem derived in ref.<sup>12)</sup>. The result is that the wave function  $U_\eta|k\rangle$  can be factorized as

$$U_\eta|k\rangle = \sum_{l \in P} U_{QL}|l\rangle \langle l|U_{VL}|k\rangle \langle c|U_\eta|c\rangle \times |\Psi_c^Q\rangle, \quad (2.3)$$

where for simplicity we denote the model-space states  $|\phi_k\rangle$  as  $|k\rangle$ . The structure of the various terms of (2.3) for  $^{18}\text{O}$  is explained in fig. 2.  $\langle c|U_\eta|c\rangle$  is the sum of the vacuum fluctuation diagrams, both linked and unlinked (fig. 2a).  $|\Psi_c^Q\rangle$  is the  $^{16}\text{O}$  eigenfunction  $U_\eta|c\rangle / \langle c|U_\eta|c\rangle$ ; some of its components are shown in fig. 2b.  $\langle l|U_{VL}|k\rangle$  represents all the diagrams starting from the model-space valence state  $k$  and ending with the model-space valence state  $l$ , with all interaction vertices linked directly or indirectly to the valence lines. These diagrams may be grouped into a  $Q(\varepsilon_k)$ -box series as indicated, with the intermediate active lines between adjacent  $Q(\varepsilon_k)$ -boxes summed over  $P$  (fig. 2c). Each  $Q(\varepsilon_k)$ -box (fig. 3) is irreducible in the sense that we may never separate any of its diagrams into two by cutting only model-space lines at equal time. We also point out each  $Q(\varepsilon_k)$  is off energy shell; that is, they depend on the initial unperturbed energy,  $\varepsilon_k(H_0|k\rangle = \varepsilon_k|k\rangle)$ .

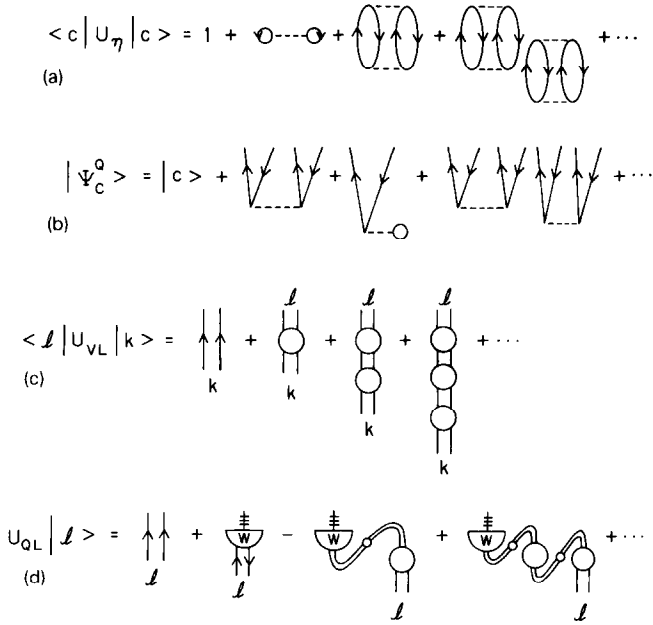


Fig. 2. Diagrams contained within the decomposition theorem for the  $^{18}\text{O}$  model-space.

The initial state  $|k\rangle$  of (2.3) belongs to the model-space  $P$ . Upon operating on  $|k\rangle$  with  $U_\eta$ , the valence particles can of course be scattered outside  $P$ . This transition is included in the term  $U_{QL}|l\rangle$  of eq. (2.3). Diagrammatically, the structure of this term is displayed in fig. 2d. The first term is the free propagation of the initial state  $k$ . The remaining terms which all undergo at least one nuclear interaction must end up in a passive state (state containing at least one passive line) at time  $t=0$ . The circular boxes are the  $Q$ -boxes mentioned earlier. The curved lines joining neighboring  $Q$ -boxes are folded<sup>12)</sup> active lines, marked by small circles. For convenience, we rewrite the graphical expression of fig. 2d as

$$U_{QL}|k\rangle = |k\rangle + \left[ W(\epsilon_k) - W \int Q(\epsilon_k) + W \int Q \int Q(\epsilon_k) + \dots \right] |k\rangle, \quad (2.4)$$

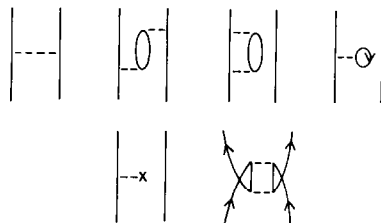


Fig. 3. Typical irreducible diagrams contained in an  $^{18}\text{O}$   $Q$ -box.



where  $P$  denotes the projection onto the model-space and  $\Delta E_\alpha = E_\alpha^{A+n_\nu} - E_0^A$ . This partial summation technique will prove useful in obtaining a convenient linked-diagram expression for the transition matrix.

### 3. Transition matrix

With the results of the preceding section, we are now ready to derive a relatively simple linked-diagram expansion for calculating the transition matrix element

$$T_{fi} = \frac{\langle \Psi_f | T | \Psi_i \rangle}{\langle \Psi_f | \Psi_f \rangle^{1/2} \langle \Psi_i | \Psi_i \rangle^{1/2}} \quad (3.1)$$

in a way which is consistent with the model-space secular equation (2.6).

We first rewrite (3.1) as

$$T_{fi} = \frac{\langle \Psi'_f | T | \Psi'_i \rangle}{\langle \Psi'_f | \Psi'_f \rangle^{1/2} \langle \Psi'_i | \Psi'_i \rangle^{1/2}} \quad (3.2)$$

with

$$|\Psi'_\alpha\rangle = \frac{|\Psi_\alpha\rangle}{\langle \rho_\alpha | \Psi_\alpha \rangle} = \frac{U_\eta(0, -\infty) |\rho_\alpha\rangle}{\langle \rho_\alpha | U_\eta(0, -\infty) | \rho_\alpha \rangle}. \quad (3.3)$$

Inserting the decomposition theorem of (2.3) for  $U_\eta(0, -\infty) |j\rangle$ , we find

$$|\Psi'_\alpha\rangle = \sum_{j \in P} U_{QL} |j\rangle \times |\Psi_c^Q\rangle b_j^\alpha, \quad (3.4)$$

where  $b$  is the model-space eigenfunction of (2.7). This is an essential step as it relates  $T_{fi}$  directly to the model-space eigenfunctions  $b$  of (2.6). Replacing the eigenfunctions  $\Psi'_f$  and  $\Psi'_i$  in (3.2) by the expansion of (3.4), we obtain immediately

$$T_{fi} = \sum_{k, l \in P} b_k^{f*} b_l^i \frac{\langle k, \Psi_c^Q | U_{QL}^\dagger T U_{QL} | l, \Psi_c^Q \rangle}{D_f D_i}, \quad (3.5)$$

where

$$D_\alpha = \left\{ \sum_{k, l \in P} b_k^{\alpha*} b_l^\alpha \langle k, \Psi_c^Q | U_{QL}^\dagger U_{QL} | l, \Psi_c^Q \rangle \right\}^{1/2}, \quad \alpha = f, i. \quad (3.6)$$

It is clear that the numerator and the denominator of  $T_{fi}$  both contain the core wave function overlap  $\langle \Psi_c^Q | \Psi_c^Q \rangle$ . These diagrams are *not* linked to either  $T$  or any valence line. However, the  $\langle \Psi_c^Q | \Psi_c^Q \rangle$  of the numerator cancels entirely with that contained in the denominator. Thus, we need only consider the linked portion of (3.5) and (3.6). Henceforth we will denote this by adding a subscript L.

It is important to note that in (3.5),  $T_{fi}$  is independent of the normalization of the  $b$  eigenvectors. Hence we may without loss of generality choose to normalize

each  $b$  vector to unity, i.e.

$$|b^\alpha|^2 \equiv \sum_{k \in P} |b_k^\alpha|^2 = 1. \tag{3.7}$$

Clearly the denominators  $D_f$  and  $D_i$  play an important role in the calculation of  $T_{fi}$  as we shall later discuss.

To understand the above results, we need to study in some detail their diagrammatic structures. For simplicity, let us consider the case of one valence nucleon outside a closed core, such as  $^{17}\text{O}$ . We also restrict ourselves for the moment to the case where the final state ( $f$ ) is different from the initial state ( $i$ ), and  $T$  is a one-body operator with its vertex denoted by  $---x$ . An example is  $\langle \Psi_f | T | \Psi_i \rangle$ , where  $T$  is the E2 transition operator, and  $\Psi_f$  and  $\Psi_i$  are different states of the nucleus  $^{17}\text{O}$ .

We note that (3.4) is in fact a rather useful and remarkable result. It states that the wave function  $\Psi'_\alpha$ , which is proportional to the true wave function  $\Psi_\alpha$ , can be rigorously expressed as a linear combination of basis functions of the form "valence wave function"  $\times$  "core wave function". In terms of diagrams, the structure of the initial state  $\Psi'_i$  is displayed in fig. 5. The structure of the final state  $\Psi'_f$  is basically identical. Let us use  $(u_i, c_i)$  and  $(u_f, c_f)$  to denote the various building blocks of the wave functions  $\Psi'_i$  and  $\Psi'_f$ , respectively, as indicated in fig. 5. With their aid we can now readily visualize the diagrammatic structure of  $T_{fi}$ .

Some typical diagrams contained in  $T_{fi}$  are displayed in fig. 6. We divide these diagrams into two categories,  $\langle k, \Psi_c^Q | U_{QL}^\dagger T U_{QL} | l, \Psi_c^Q \rangle \equiv N_{kl}$  and  $\langle k, \Psi_c^Q | U_{QL}^\dagger U_{QL} | l, \Psi_c^Q \rangle \equiv D_{kl}$ . We first consider  $N_{kl}$ . Clearly, diagram (i) of fig. 6 belongs to  $N_{kl}$  and originates from  $\langle u_f(1) | T | u_i(1) \rangle \langle \Psi_c^Q | \Psi_c^Q \rangle$ , and similarly diagram (ii) comes from  $\langle u_f(2) | T | u_i(2) \rangle \langle \Psi_c^Q | \Psi_c^Q \rangle$ . As discussed earlier, the factor  $\langle \Psi_c^Q | \Psi_c^Q \rangle$  is common to both  $N_{kl}$  and  $D_{kl}$  and they cancel with each other. Therefore, from now on we will omit this factor for both  $N_{kl}$  and  $D_{kl}$ . Diagram (iii) is a twice folded diagram coming from  $\langle u_f(4) | T | u_i(4) \rangle$ . There are also mixed terms such as diagram (iv) coming from  $\langle u_f(1) | T | u_i(3) \rangle$ .

The structure of the diagrams belonging to  $D_{kl}$  is identical to  $N_{kl}$  except for the replacement of  $T$  by the unit operator 1. For example, diagram (v) which belongs

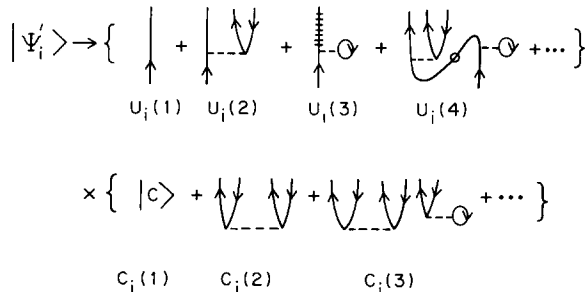


Fig. 5. Typical diagrams involved in the linked expansion of  $|\Psi_i\rangle$ .

to  $D_{kl}$  comes from  $\langle u_f(2)|1|u_i(2)\rangle$ , the horizontal line in the middle denotes the unit transition operator and it has the consequence that the energy denominators just above and below the line are identical to each other. It is clear that (v) is a wavefunction overlap diagram.

In general, there are also diagrams with  $T$  attached to the core wave functions. An example is diagram (vi) of fig. 6 which originates from  $\langle c_f(2)|T|c_i(2)\rangle$ . Diagrams of this type are, however, non-zero only when  $T$  is a scalar operator and  $f=i$ , i.e. such diagrams are non-zero only when evaluating the expectation value of scalar operators. Finally, there are also valence-core mixed diagrams as shown by diagram (vii). This diagram comes from  $\langle u_f(2)|T|u_i(1)c_i(2)\rangle$ .

It may be helpful to describe some physical interpretations. Diagram (ii) for instance may be referred to as a core polarization correction. It means that the eigenstate of  $^{17}\text{O}$  has also  $2p1h$  admixtures in addition to the  $1p0h$  component. Diagram (ii) represents the contribution of these admixtures to  $T_{fi}$ . Note that the  $T$  vertex is always located at time  $t=0$ . As an illustration, the contribution of this diagram is

$$d(\text{ii}) = \frac{(-1)^3}{2} \sum_{\substack{1,2 > k_F \\ 3,4 < k_F}} \frac{\langle k3|V|12\rangle\langle 4|T|3\rangle\langle 12|V|l4\rangle}{[\epsilon_k - (\epsilon_1 + \epsilon_2 - \epsilon_3)][\epsilon_l - (\epsilon_1 + \epsilon_2 - \epsilon_4)]}, \quad (3.8)$$

where  $V$  denotes the NN interaction. Diagram (iii) is a twice-folded diagram. As

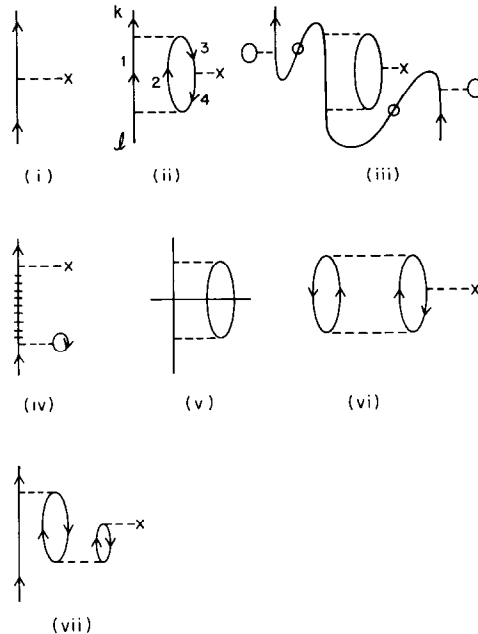
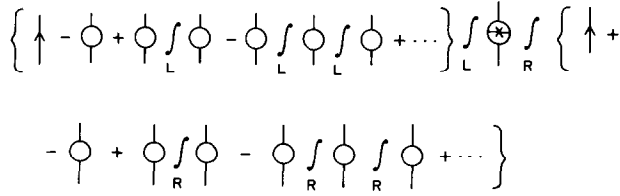


Fig. 6. Typical diagrams contained in  $\langle k|U_{QL}TU_{QL}|l\rangle_1 \equiv N_{kl}$  and  $\langle k|U_{QL}^+U_{QL}|l\rangle_1 \equiv D_{kl}$ .

Fig. 7. General structure of  $N_{kl} \equiv \langle k | U_{QL} T U_{QL} | l \rangle_L$ .

we shall see shortly, this type of diagram has the effect of “renormalizing” the starting energies of the non-folded diagrams such as diagram (ii).

In fig. 7, we display the general structure of  $N_{kl}$ . As shown, it can have any number of L- and R-folds. It would seem to be rather cumbersome to calculate these folds. Fortunately, considerable simplification can be achieved by applying the partial summation method of Krenciglowa and Kuo<sup>17)</sup> to  $N_{kl}$  and  $D_{kl}$ . Using this method, it is straightforward to show that the transition matrix formula becomes

$$T_{fi} = \sum_{k,l \in P} b_k^{f*} b_l^i \frac{\langle k, \Psi_c^Q | \{1 + W^\dagger(\Delta E_f)\} T \{1 + W(\Delta E_i)\} | l, \Psi_c^Q \rangle_L}{D_f D_i} \quad (3.9)$$

with

$$D_\alpha = \left\{ 1 + \sum_{k,l \in P} b_k^{\alpha*} b_l^\alpha \langle k, \Psi_c^Q | W^\dagger(\Delta E_\alpha) W(\Delta E_\alpha) | l, \Psi_c^Q \rangle_L \right\}^{1/2}, \quad \alpha = f, i. \quad (3.10)$$

Note that in the above, we have used the normalization of (3.7).

The above results are considerably simpler for calculation than (3.5) and (3.6). We no longer have to calculate any folded diagrams. In (3.9) and (3.10) we just calculate the non-folded wave function box at the eigenenergies  $\Delta E_i$  and  $\Delta E_f$  obtained from the model-space secular equation (2.6) or (3.8). (As an example, diagram (ii) of fig. 6 is given presently also by (3.8) except for the replacement of  $\varepsilon_k$  by  $\Delta E_f$  and  $\varepsilon_l$  by  $\Delta E_i$ .) We note that the diagrams chosen to be contained in the wave function box  $W$  should be consistent with those included in the calculation of the effective interaction  $V^{\text{eff}}$  used in (2.6). This is because the operator  $U_{QL}$  which enters the calculation of  $T_{fi}$  also enters the calculation of  $V^{\text{eff}}$  [ref. 12)].

The calculation of  $D_\alpha$  may be simplified. By inspection, one sees that the wave function overlap diagrams,  $\langle k, \Psi_c^Q | W^\dagger(\Delta E_\alpha) W(\Delta E_\alpha) | l, \Psi_c^Q \rangle_L$ , have the same topological structure as those in the  $Q$ -box. Numerically, they are however different as every diagram of  $\langle k, \Psi_c^Q | W^\dagger(\Delta E_\alpha) W(\Delta E_\alpha) | l, \Psi_c^Q \rangle_L$  contains one propagator squared. An example is diagram (v) of fig. 6 as discussed earlier. In fact it is straightforward to verify that

$$\langle k, \Psi_c^Q | W^\dagger(\Delta E_\alpha) W(\Delta E_\alpha) | l, \Psi_c^Q \rangle_L = - \frac{d}{d\omega} \langle k | Q(\omega) | l \rangle \Big|_{\omega = \Delta E_\alpha}, \quad \alpha = f, i. \quad (3.11)$$

From (2.9) we may define an energy-dependent function

$$\mathcal{E}_\alpha(\omega) = \frac{\langle P\Psi_\alpha | [H_0 + Q(\omega)] | P\Psi_\alpha \rangle}{\langle P\Psi_\alpha | P\Psi_\alpha \rangle} \quad (3.12)$$

which has the property

$$\mathcal{E}_\alpha(\Delta E_\alpha) = \Delta E_\alpha, \quad (3.13)$$

with  $\Delta E_\alpha^{A+n} = E_\alpha^{A+n} - E_0^A$ . We then obtain from (3.10) and (3.11)

$$D_\alpha^2 = 1 - \left. \frac{d}{d\omega} \mathcal{E}(\omega) \right|_{\omega = \Delta E_\alpha} \equiv \frac{1}{\mathcal{N}_\alpha}. \quad (3.14)$$

From the above we have our final expression for the transition matrix as

$$T_{fi} = (\mathcal{N}_f \mathcal{N}_i)^{1/2} \sum_{kl \in P} b_k^{f*} b_l^i \langle k, \Psi_c^Q | \{1 + W^\dagger(\Delta E_f)\} T \{1 + W(\Delta E_i)\} | l, \Psi_c^Q \rangle_L, \quad (3.15)$$

where L signifies that only the valence-linked diagrams are retained. (3.15) is the principal result of this work. It is directly analogous to the reduction formula of field theory<sup>18</sup>). As in the reduction formula, (3.15) contains only (non-folded) linked diagrams. The  $\mathcal{N}$  factors are the renormalization factors of the ‘‘external’’ lines, while the partial summation of the folded diagrams allows us to calculate diagrams at the physical energies of the initial and final states i.e. the initial and final states are on-shell. This similarity with the reduction formula in field theories is both interesting and surprising considering that (3.15) is derived for bound-state transition amplitudes, while the reduction formula is derived within the context of collision theory.

The  $\mathcal{N}$  factors may play an important role in the calculation of the transition matrix element  $T_{fi}$  of (3.15). It is of interest that we can actually use this equation to study the physical meaning of the  $\mathcal{N}$  factor itself. The above formulation is valid for operators which do not conserve the number of particles. An example is  $T = a_i a_j$ ,  $i$  and  $j \in P$ . Let us consider the transition matrix element of this operator between the states  $\Psi_0^A$  and  $\Psi_\alpha^{A+2}$ . This transition matrix element can be derived following essentially the same steps which lead to (3.15). The initial state now has two valence particles and its wave function corresponding to (3.4) is written as

$$|\Psi_\alpha'(A+2)\rangle = \sum_{m,n \in P} U_{QL} |m, n\rangle \times |\Psi_c^Q\rangle b_{mn}^\alpha, \quad (3.16)$$

where  $m$  and  $n$  denote single-particle states for the valence particles. The final state is a closed-core state, i.e.

$$|\Psi_0'(A+2)\rangle = \frac{U_\eta(0, -\infty)|c\rangle}{\langle c|U_\eta(0, -\infty)|c\rangle} \quad (3.17)$$

which is just the state  $\Psi_c^Q$ . Here  $c$  denotes the unperturbed core state. Substituting the above into (3.2) readily leads to a result similar to (3.9). Clearly it does not

contain the factors  $\mathcal{N}_f$ ,  $b_f$  and  $W^\dagger(\Delta E_f)$  because the final state is a closed-core state. Since  $i$  and  $j$  are within  $P$  while  $W$  always leads to states outside  $P$ , we have  $\langle \Psi_c^Q | a_i a_j \{1 + W(\Delta E_i)\} | mn, \Psi_c^Q \rangle_L = \delta_{ij, mn}$ . Thus this matrix element is obtained as

$$\langle \Psi_0^A | a_i a_j | \Psi_\alpha^{A+2} \rangle = b_{ij}^\alpha \mathcal{N}_\alpha^{1/2} \quad (3.18)$$

where  $i$  and  $j$  belong to the model space. Since in our formalism the  $b$  vector is normalized to 1, the above implies

$$\sum_{i > j \in P} |\langle \Psi_0^A | a_i a_j | \Psi_\alpha^{A+2} \rangle|^2 = \mathcal{N}_\alpha. \quad (3.19)$$

This is a rather interesting result. It tells us that  $\mathcal{N}_\alpha$ , which can be evaluated using (3.14), is a direct measure of the overlaps  $\langle \Psi_0^A | a_i a_j | \Psi_\alpha^{A+2} \rangle$ . The need of having wave-function normalizations in the calculation of transition matrix elements has been emphasized by a number of authors<sup>1-11</sup>), but a systematic prescription for calculating them in strict consistency with the underlying effective interaction theory seems to have not been given before the present work. Brandow has considered the normalization of the entire wave function, such as  $\langle \Psi_\alpha^{A+2} | \Psi_\alpha^{A+2} \rangle$ , and has given similar expressions<sup>11</sup>), but here our normalization is specifically for the transition amplitudes as indicated by eq. (3.19). Our present result is probably most similar to that of ref.<sup>19</sup>) where the normalization of the transition amplitudes involving both the  $(A+2)$  and  $(A-2)$  system was studied jointly, using a Green function approach.

From (3.14), we see that the  $\mathcal{N}$  factors may be calculated from the slope of  $\mathcal{E}_\alpha(\omega)$ . It should be of interest to actually perform a calculation for such normalization factors, to have a feeling for their importance. We have carried out such a calculation for the low-lying states of  $^{18}\text{O}$  and  $^{18}\text{F}$ , using a  $G$ -matrix effective interaction derived from the Paris nucleon-nucleon potential<sup>20</sup>). Our main purpose is to determine the magnitude of the  $\mathcal{N}_\alpha$  factors for these states. The bare  $G$ -matrix is calculated using a momentum space matrix inversion method which treats the Pauli exclusion operator essentially exactly; in fact, we used a Pauli exclusion operator specified by  $(n_1, n_2, n_3) = (3, 6, 21)$  [ref.<sup>21</sup>)]. In the  $Q$ -box, we include the two- and one-body diagrams first- and second-order in the  $G$ -matrix, namely the two-body diagrams ( $G, G_{3p1h}, G_{2p}, G_{2h}$ ) and the one-body ones ( $G, G_{2p1h}, G_{2h1p}$ ). The calculation of these diagrams was described for example in ref.<sup>22</sup>). In figs. 8 and 9, we plot  $\mathcal{E}_\alpha(\omega)$  for the low-lying states of  $^{18}\text{O}$  and  $^{18}\text{F}$ , respectively. The self-consistent energies are given by the positions of the intersection points between the curves and the  $45^\circ$  line. Now, however, we note that the slopes at the self-consistency point also carry physical significance and they allow us to determine the corresponding  $\mathcal{N}$  factor of (3.19). Actually these slopes turned out to be rather large.

In figs. 10 and 11, we list the  $\mathcal{N}$  factors, in parenthesis, for the various low-lying states of  $^{18}\text{O}$  and  $^{18}\text{F}$ . Their values are typically about 0.75. This is significant as this means according to (3.19), that the wave function  $|\Psi_\alpha^{A+2}\rangle$  has a rather large

Paris ( $^{18}\text{O}$ )

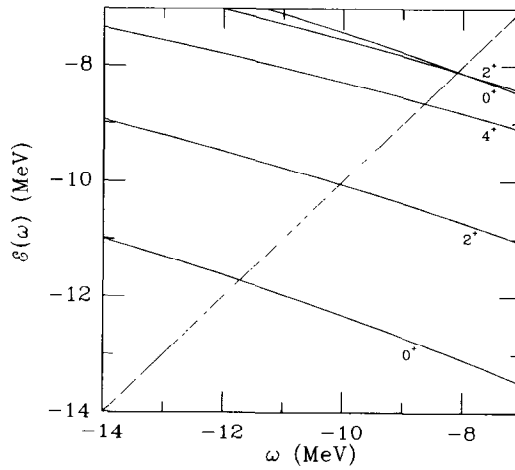


Fig. 8.  $\mathcal{E}_\alpha(\omega)$  for  $^{18}\text{O}$  (see eq. (3.12)).

portion which lies outside the model space  $P$ . In figs. 10 and 11 we also compare our calculated energy spectra with experiment.

A word of caution to the reader here. Although our results achieve some success in reproducing the experimental spectrum, we should keep in mind that our calculation is merely a low-order one. We include in our  $Q$ -box only diagrams first and

Paris ( $^{18}\text{F}$ )

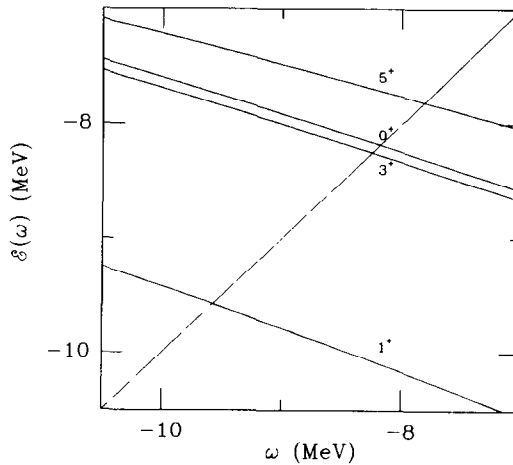
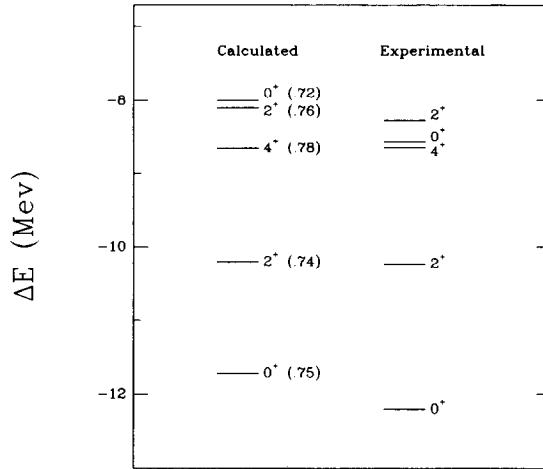
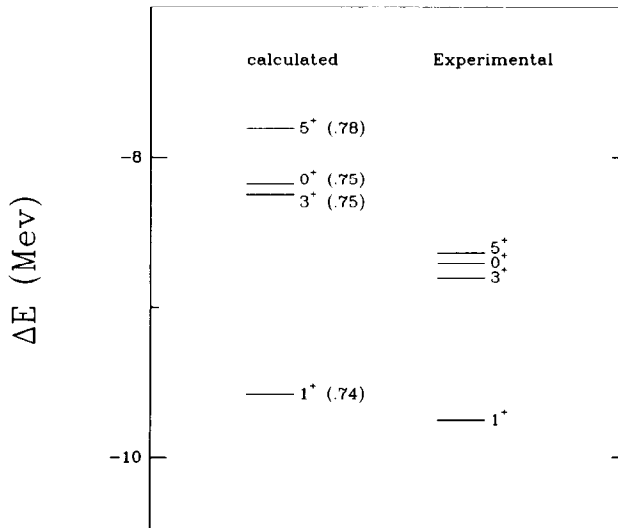


Fig. 9.  $\mathcal{E}_\alpha(\omega)$  for  $^{18}\text{F}$  (see eq. (3.12)).

Paris ( $^{18}\text{O}$ )Fig. 10.  $^{18}\text{O}$  energy level; normalization factors in parentheses.Paris ( $^{18}\text{F}$ )Fig. 11.  $^{18}\text{F}$  energy levels; normalization factors in parentheses.

second order in the  $G$ -matrix interaction. Then a self-consistent calculation, see eq. (2.9), based on this  $Q$ -box is performed to determine the energies as well as the  $\mathcal{N}_\alpha$  factors. This self-consistent calculation is equivalent<sup>17)</sup> to a summation of the folded-diagram  $Q$ -box series to all orders using an iterative partial summation method. Higher order diagrams not included in the present work remain to be investigated. They may significantly affect our present results. But, nevertheless, our present low-order calculation does seem to indicate that the  $\mathcal{N}_\alpha$  factors can be significantly different from unity and thus may provide important normalization corrections to the calculated decay rates. Intruder states have played a central role in effective interaction and operator theories<sup>23,24)</sup>. There is considerable evidence, see e.g. ref.<sup>25)</sup>, that the first excited  $2^+$  and the first excited  $0^+$  states are “intruder” states with large  $4p2h$  components. The *energies* of these states are, however, reasonably well reproduced by our present calculation and by earlier similar  $G$ -matrix calculations of Kuo and Brown<sup>26)</sup> and Shurpin *et al.*<sup>22)</sup>. This is a puzzling situation and should be further investigated. Model calculations<sup>16,17)</sup> have demonstrated that the energies given by the folded diagram partial summation method, which is basically the same as the method employed here, usually converge to the states with the largest  $P$ -space overlaps whether they are intruder states or not. A Taylor series expansion of  $V^{\text{eff}}$  in powers of the coupling constant does not converge, in general, in the presence of intruder states, although model calculations have shown that Padé approximations may be useful in circumventing this divergence problem<sup>27)</sup>.

However, the  $V^{\text{eff}}$  used here is not based on a Taylor series expansion. A likely scenario is that our present calculation may be able to reproduce the energies of the excited states reasonably well, but not so for their wave-functions and associated transition rates. For them, one probably must treat the intruder-state components explicitly. A further study along this direction should be most worthwhile. This is, however, beyond the scope of our present work and we hope to carry out such a study in the near future. In passing, we mention that Jorth-Jensen and Osnes<sup>28)</sup> have recently addressed the convergence problem of realistic effective interactions with emphasis on the third-order  $Q$ -box diagrams.

For a general case with  $n_v$  valence particles (3.19) generalizes to

$$\sum_{l\dots m, i\dots j \in P} |\langle \Psi_0^A | \underbrace{a_l^\dagger \dots a_m^\dagger}_{n_h} \underbrace{a_i \dots a_j}_{n_p} | \Psi_\alpha^{A+n_v} \rangle|^2 = \mathcal{N}_\alpha. \quad (3.20)$$

Finally we add that our formulation applies to expectation values as well, readily yielding

$$\begin{aligned} \langle \Psi_\alpha | A | \Psi_\alpha \rangle &= \langle \Psi_c^Q | A | \Psi_c^Q \rangle_L \\ &+ \mathcal{N}_\alpha \sum_{k \in P} b_k^{\alpha*} b_k^\alpha \langle k, \Psi_c^Q | \{1 + W^\dagger(\Delta E_\alpha)\} A \{1 + W(\Delta E_\alpha)\} | k, \Psi_c^Q \rangle_L. \end{aligned} \quad (3.21)$$

If  $\Psi_\alpha$  is the ground state  $\Psi_0$ , the above reduces to the well known linked-diagram expansion  $\langle \Psi_0 | A | \Psi_0 \rangle = \langle \Psi_c^Q | A | \Psi_c^Q \rangle_L$  containing only linked-diagrams with one  $A$  vertex<sup>6</sup>).

#### 4. Conclusion

The main result of the present work is (3.15) which provides a unified and relatively simple method for calculating the transition matrix element  $T_{fi}$ . One first derives the effective interaction  $V^{\text{eff}}$  and solves the model-space secular equation (2.6). This equation does not determine the normalization of the model-space eigenvectors  $b^\alpha$ . We have shown that we can choose to normalize these vectors each to unity provided that in calculating  $T_{fi}$ , the wave-function normalization factors  $\mathcal{N}_f$  and  $\mathcal{N}_i$  are also included.

The need of having such wave-function normalization factors has been studied in the past, but their calculation would be rather difficult. We have derived a much simpler way to evaluate these factors, within the framework of a linked-diagram formalism. As shown by (3.14), they are simply given in terms of the respective energy derivative of the self-consistent model-space eigenvalue. Our result is in fact rather similar to the normalization of the Green function transition amplitudes of ref.<sup>19</sup>).

It should be of much interest to calculate matrix elements with this formalism, which we plan to do in the near future. It is likely that these factors will turn out to be significantly smaller than one, which would considerably suppress the transition matrix element. This may have some important consequences. As is well known, a number of recent nuclear structure calculations have given the calculated transition rates as being too large compared with the experimental values. This has brought up various proposals of quenching mechanisms, such as the  $\Delta$ -hole admixture in the nuclear wave functions, for the purpose of suppressing the calculated transition rates. [See, for example, refs.<sup>29,30</sup>) and the references quoted therein.] It seems that in earlier calculations no serious attempt has been given to the calculation and the inclusion of the wave-function normalization factors. The inclusion of these factors in the calculation of  $T_{fi}$  is likely to provide a significant portion of the needed quenching effect. If this turns out to be the case, the need of other quenching mechanisms may be considerably reduced.

We emphasize that there is a compensating factor which has to be taken into account. The  $\mathcal{N}$  factors in (3.15) would most likely have a suppressing effect on  $T_{fi}$ , but the contribution to  $T_{fi}$  from the wave-function components which lie outside the model-space may have an enhancing effect on  $T_{fi}$ . This contribution, referred to as the  $Q$ -space contribution, enters  $T_{fi}$  via the wave-function boxes  $W$  and the core wave-function  $\Psi_c^Q$  of (3.15). In fact our formulation provides a self-consistent scheme for determining which linked-diagrams should be included in  $T_{fi}$ . The starting point is the effective interaction  $V^{\text{eff}}$  of (2.6). Once one has decided which

diagrams should be included in  $T_{fi}$ , the quantities  $\mathcal{N}$ ,  $b$ , and  $\Delta E$  are all fixed accordingly. Since there is a definite relation between the diagrams included in  $V^{\text{eff}}$  and those contained in  $W$  and  $\Psi_c^Q$ , the diagrams to be included in the  $Q$ -space contribution to  $T_{fi}$  are entirely determined by the way we choose to calculate  $V^{\text{eff}}$ . This is a main point of our result.

In practically all shell-model calculations, the transition matrix element  $T_{fi}$  is calculated as  $\sum_{kl \in P} \chi_k^{I*} \chi_l^I \langle k | T^{\text{eff}} | l \rangle$  where the  $\chi$ 's are the shell-model wave functions.  $T^{\text{eff}}$ , as mentioned earlier is an effective transition operator usually determined in an empirical way. This shell-model  $T_{fi}$  is rather different from that given by (3.15), the former essentially corresponding to the latter with the  $\mathcal{N}$  factors set to 1,  $\Psi_c^Q$  and  $W$  both ignored, and  $T^{\text{eff}}$  replaced by  $T$ . To a large extent, the empirical shell-model effective interaction can now be derived from a realistic nucleon-nucleon interactions using the method outlined in sect. 2<sup>26-32</sup>). Hence the wave functions  $b$  and  $\chi$  should be rather close to each other, but the other aspects of these two means of computing  $T_{fi}$  are really quite different. It should be of much interest as well as useful to carry out calculations using both methods and compare their results.

The reader may have noticed that while we started out with a Raleigh-Schrodinger type perturbation theory, what has been accomplished is basically a synthesis of Raleigh-Schrodinger and Brillouin-Wigner valence-linked perturbation theory in an attempt to extract desirable properties of each. We note that our formalism for  $T_{fi}$  does not require the calculation of any folded diagrams which is a convenience compared with earlier methods.

The authors are obliged to S.S. Wu and P.J. Ellis for helpful discussions.

## References

- 1) I.S. Towner, A shell model description of light nuclei (Clarendon, Oxford, 1977), ch. 5; see also references quoted therein
- 2) P.J. Ellis and E. Osnes, Rev. Mod. Phys. **49** (1977) 777
- 3) M. Harvey and F.C. Khana, Nucl. Phys. **A152** (1970) 588
- 4) H.A. Weidenmuller, Ann. of Phys. **96** (1976) 139
- 5) J.M. Leinaas and T.T.S. Kuo, Ann. of Phys. **98** (1976) 177
- 6) E.M. Krenciglowa and T.T.S. Kuo, Nucl. Phys. **240** (1975) 195
- 7) T.T.S. Kuo and E. Osnes, Phys. Rev. **C12** (1975) 309
- 8) E.M. Krenciglowa, T.T.S. Kuo, E. Osnes and P.J. Ellis, Nucl. Phys. **A289** (1977) 281
- 9) S. Siegel and L. Zamick, Nucl. Phys. **A145** (1970) 89
- 10) P. Federman and L. Zamick, Phys. Rev. **177** (1969) 1534
- 11) B.H. Brandow, Rev. Mod. Phys. **39** (1976) 771
- 12) T.T.S. Kuo, S.Y. Lee and K.F. Ratcliff, Nucl. Phys. **A176** (1971) 65
- 13) T.T.S. Kuo, Ann. Rec. Nucl. Sci. **24** (1974) 101
- 14) M. Gell-Mann and F. Low, Phys. Rev. **84** (1951) 350
- 15) D.J. Thouless, The quantum mechanics of many-body systems (Academic Press, New York, 1961)
- 16) T.T.S. Kuo, Lecture Notes in Physics **144** (1981) 248
- 17) E.M. Krenciglowa and T.T.S. Kuo, Nucl. Phys. **A235** (1974) 171
- 18) C. Itzykson and J.B. Zuber, Quantum field theory (McGraw-Hill, New York, 1961)

- 19) S.D. Yang and T.T.S. Kuo, Nucl. Phys. **A456** (1986) 413
- 20) R. Vinh-Mau, in Mesons in nuclei, ed. M. Rho and D. Wilkenson (North-Holland, Amsterdam, 1979) p 151
- 21) E.M. Krenciglowa, C.L. Kung, T.T.S. Kuo and E. Osnes, Ann. of Phys. **101** (1976) 154
- 22) J. Shurpin, T.T.S. Kuo and D. Strottman, Nucl. Phys. **A408** (1983) 310
- 23) H.M. Hoffman, S.Y. Lee, J. Richert, H.A. Weidenmuller and T. Schuan, Ann. Phys. **85** (1974) 410
- 24) H.A. Weidenmuller, in Int. Topical Conf. on Effective interactions and operators, ed. H.P. Blok and A.E.L. Dieperink, vol. 40 (Springer, Berlin, 1975)
- 25) G.E. Brown and A.M. Green, Nucl. Phys. **85** (1966) 86
- 26) T.T.S. Kuo and G.E. Brown, Nucl. Phys. **85** (1966) 40
- 27) H.M. Hoffman, S.Y. Lee, J. Richert, H.A. Weidenmuller and T. Schuan, Phys. Lett. **B45** (1973) 421
- 28) M. Jorth-Jensen and E. Osnes, Phys. Lett. **B228** (1989) 281  
Phys. Scripta **41** (1990) 207
- 29) I. Towner, Phys. Reports **155** (1987) 263
- 30) W. Weise, Prog. Part. Nucl. Phys. **11** (1984) 123
- 31) B.H. Wildenthal, Prog. Part. Nucl. Phys. **11** (1984) 5
- 32) T.T.S. Kuo, in Second Int. Seminar on nuclear physics, Capri, Italy, ed. A. Covello (World Scientific, Singapore, 1988) p 29